J Appl Electrochem
DOI 10.1007/s10800-014-0729-4

RESEARCH ARTICLE

Corrosion inhibition of mild steel in sulphuric acid using a bicyclic thiadiazolidine

Mauro J. Banera · José A. Caram · Claudio A. Gervasi · María V. Mirífico

Received: 18 June 2014 / Accepted: 11 August 2014

Abstract The inhibitory effect of 3a,6a-diphenyltetrahydro-1H-imidazo [4,5-c] [1, 2, 5] thiadiazole-5(3H)-thione 2,2-dioxide (TTU) on the corrosion behaviour of mild steel in 0.5 M H_2SO_4, at (30 ± 0.5) °C was studied by gravimetric, potentiodynamic polarization, electrochemical impedance spectroscopy, and scanning electron microscopy measurements. The effect of inhibitor concentration on the corrosion rate, surface coverage and inhibition efficiency is investigated. Results show that TTU exerts a strong inhibiting effect on mild steel corrosion and acts as a cathodic-type inhibitor. TTU does not affect the mechanism of the cathodic reaction while the anodic reaction mechanism changes upon addition of the inhibitor. Possible mechanistic pathways for the inhibition process are proposed. The inhibition efficiency of TTU may be due to either the adsorption of inhibitor molecules building a protective film or the formation of an insoluble complex of the inhibitor with metal cations. TTU adsorption obeys the Langmuir model.

M. J. Banera · J. A. Caram · C. A. Gervasi (✉) · M. V. Mirífico (✉)
Departamento de Química, Facultad de Ciencias Exactas, Instituto de Investigaciones Fisicoquímicas Teóricas y Aplicadas (INIFTA, CCT La Plata-CONICET), Universidad Nacional de La Plata, Casilla de Correo 16, Sucursal 4, 1900 La Plata, Argentina
e-mail: gervasi@inifta.unlp.edu.ar

M. V. Mirífico
e-mail: mirifi@inifta.unlp.edu.ar

C. A. Gervasi · M. V. Mirífico
Departamento de Ingeniería Química, Facultad de Ingeniería, UNLP, 1 y 47, 1900 La Plata, Argentina

Keywords Acid inhibition · Imidazolidine-2-thione · Weight loss · EIS · Potentiodynamic polarization

1 Introduction

The main objective of applying the acid pickling process (i.e., removal of oxide and other scales from the surface) to steel products is the elimination of irregular conditions and the promotion of surface smoothness of the finished product. Consequently, pickling is usually the previous step to hot-dip coating or electroplating [1]. As acidic media, hydrochloric acid (HCl) and sulphuric acid (H_2SO_4) are often used as industrial acid cleaners and pickling acids [2]. However, since the acid also reacts with the base steel, an inhibitor is usually added to the acid solution to inhibit or lessen this acid attack on the steel itself while allowing preferential removal of the iron oxides [3]. The distinction between acid cleaning and acid pickling is a matter of degree, with acid cleaning as a less severe treatment for final or near-final preparation of metal surfaces before plating, painting, or storage. Acid solutions of 40–60 %vol hydrochloric or 6–8 %vol sulphuric (often containing up to 1 % inhibitor) are used at room temperature for removing soil and light rust.

Among the most important organic corrosion inhibitors for acid media, heterocyclic compounds containing endocyclic and/or exocyclic N, S, O atoms are considered to be the most effective [2]. Noteworthy, the inhibition efficiency of N-heterocyclic organic inhibitors increases with the number of aromatic systems and the availability of electronegative atoms in the molecule [4]. Therefore, this work aims at studying the inhibitory effect of a novel N-heterocyclic compound first synthesized in our laboratory [5] on the corrosion of mild steel in 0.5 M H_2SO_4, at (30 ± 0.5) °C.

Published online: 21 August 2014

2 Experimental

2.1 Inhibitor

The inhibitor 3a,6a-diphenyltetrahydro-1H-imidazo[4,5-c] [1, 2, 5] thiadiazole-5(3H)-thione 2,2-dioxide (TTU) was synthesized according to the procedure proposed by us [5]. Figure 1 shows the molecular structure of this compound. The inhibitor is a bis (N-heterocyclic) molecule containing sulphur and oxygen. In this molecule four nitrogen atoms (>N–H) and one sulphur atom (>C=S) are potentially capable of acting as the main active centres of adsorption [6–8]. It is well known that the heterocyclic thione donors have a wide range of applications that include metallic corrosion inhibition [7, 9].

The concentration range of the inhibitor was 30–120 μM in the corrosive medium.

2.2 Specimens and electrolytes

Composition of mild steel (percent by mass) was as follows: C-0.21; Mn-0.9; P-0.022; Si-0.03; S-0.030; Cr-0.11; Ni-0.12; Mo-0.022; Al-0.07; Cu-0.15 and the balance Fe.

Steel samples were wet-ground with silicon carbide abrasive papers (grades #400 to #1000) and then thoroughly ultrasonically rinsed with MilliQ® water, ultrasonically degreased with acetone, and finally, dried with a warm air stream immediately before use. The corrosive solution used was prepared with H_2SO_4 AR (Merck Química Argentina SAIC, BA, Argentina) and MilliQ® water.

2.3 Gravimetric measurements

Weight loss experiments were conducted on test coupons of size 3.0 cm × 3.0 cm × 0.14 cm. Specimens were prepared immediately before use as described above (see Sect. 2.2). Cleaned weighed coupons were freely suspended in glass reaction vessels containing the test solutions. Experiments were performed under total immersion conditions in 250 mL of 0.5 M H_2SO_4 naturally aerated and unstirred, without and with the addition of TTU in different concentrations. Solutions were kept at (30 ± 0.5) °C using a thermostated water bath. To determine weight loss, coupons were removed after 24 h of immersion, placed in 20 %w/v NaOH solution containing 200 g/L of zinc dust, scrubbed with a bristle brush, washed with copious amounts of water and then with acetone, dried, and weighed. The difference between the weight after immersion and initial weight corresponds to the weight loss. Experiments were performed in triplicate to verify reproducibility of results. Triplicate determinations showed good reproducibility, which was greater than 95 %.

2.4 Electrochemical measurements

Steel samples for electrochemical experiments were machined into cylindrical specimens and then embedded in polytetrafluoroethylene (PTFE) with an exposed geometrical area of 0.283 cm^2. The exposed surface was also cleaned as described above (see Sect. 2.2). Electrochemical experiments were conducted in a three-electrode electrochemical cell using a Zahner IM6 electrochemical workstation. A platinum sheet was used as the counter electrode, and a saturated calomel electrode (SCE) was used as the reference. All potentials in this work are referred to the SCE (0.2,411 V with respect to the standard hydrogen electrode). Measurements were performed in naturally aerated and unstirred solutions at the end of 24 h of immersion at 30 ± 0.5 °C, controlled using a thermostated water bath. Impedance measurements were carried out at the corrosion potential (E_{corr}) over a frequency range from 50 kHz to 100 mHz, with a perturbation signal amplitude of 10 mV. Potentiodynamic polarization experiments were conducted in the potential range between −100 and +100 mV versus E_{corr} at a scan rate of 0.2 mV s^{-1}. Each test was run in triplicate to verify the reproducibility of results.

2.5 SEM surface analysis

Morphological studies of the mild steel samples were undertaken by scanning electron microscope (SEM) examinations of surfaces exposed to different test solutions, using a Quanta 200 (FEI, Holland) SEM operating with a tungsten filament as the electron source. Mild steel specimens of size 3.0 cm × 3.0 cm × 0.14 cm were ground as described above (see Sect. 2.2) and thereafter polished using a cloth with 5μm diamond paste to obtain a near mirror-like finish on the surface. Samples were subsequently immersed for 24 h in the blank solution (0.5 M H_2SO_4) without and with 120 μM TTU at (30 ± 0.5) °C, and finally, they were washed with distilled water, dried in warm air, and submitted for SEM surface examination.

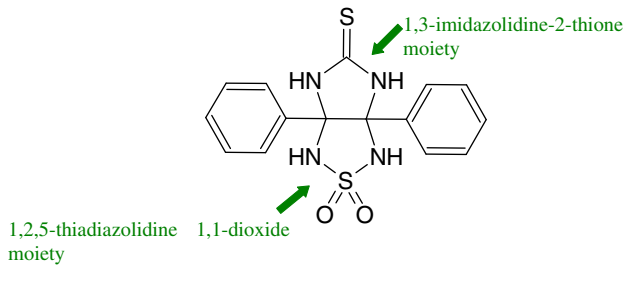

Fig. 1 Molecular structure of 3a,6a-diphenyltetrahydro-1H-imidazo[4,5-c] [1, 2, 5]thiadiazole-5(3H)-thione 2,2-dioxide (TTU)

Table 1 Corrosion rates and inhibition efficiencies of mild steel in 0.5 M H_2SO_4 with different concentrations of TTU as obtained from weight loss measurements

Concentration of TTU (μM)	v (mg cm^{-2} h^{-1})	$\%\eta$	θ
0	0.454	–	–
30	0.093	79.6	0.796
60	0.042	90.6	0.906
90	0.039	91.3	0.913
120	0.030	93.4	0.934

3 Results and discussion

3.1 Corrosion inhibition evaluation

3.1.1 Gravimetric measurements

From weight loss values, corrosion rates (v) were computed using Eq. 1.

$$v = (m_1 - m_2)/A \times t \quad (1)$$

where m_1 and m_2 are weights (mg) of mild steel coupons before and after immersion in test corrosive solutions, respectively, A is the exposed area of a specimen (cm^2) and t is the immersion time (h).

The inhibition efficiency ($\%\eta$) of TTU was evaluated from Eq. (2).

$$\%\eta = 100 \times (v_0 - v)/v_0 \quad (2)$$

where v_0 and v are the corrosion rates in 0.5 M H_2SO_4 in the absence and presence of the inhibitor, respectively, at the experimental temperature.

Values for $\%\eta$ and v for mild steel in 0.5 M H_2SO_4 without and with different concentrations of TTU, at 30°C are shown in Table 1. Reported results correspond to average values.

Assuming that η is a direct measure of the degree of surface coverage (θ), Eq. 3 can be used to estimate this value for the different concentrations of TTU from weight loss data.

$$\theta = \%\eta/100 \quad (3)$$

Results in Table 1 indicate that the corrosion rate decreases after the addition of TTU when compared with the blank solution (0.5 M H_2SO_4) and that TTU acts as an efficient corrosion inhibitor. Moreover, corrosion rate decreases markedly after changing TTU concentration from 0 to 30 μM. However, above this TTU concentration, further decrease in corrosion rate becomes less marked. A decrease in corrosion rate in the presence of TTU corresponds to an increase in inhibition efficiency (Eq. (2)). Inspection of data in Table 1 reveals that $\%\eta$ increases markedly in the presence of 30 μM TTU when compared with the blank solution. However, for higher TTU concentrations the increase in inhibition efficiency becomes less pronounced. This behaviour indicates that TTU acts as an effective inhibitor even at low concentrations. Corrosion inhibition is thought to be initiated by the displacement of adsorbed water molecules by the inhibitor species that leads to the specific adsorption of the inhibitor on the metal surface [10]. Heteroatoms (N, O and exocyclic S) with lone pair electrons and possibly aromatic rings with π-electrons, may donate electrons to the vacant d-orbital of Fe atoms, and as a result, the adsorption of TTU takes place.

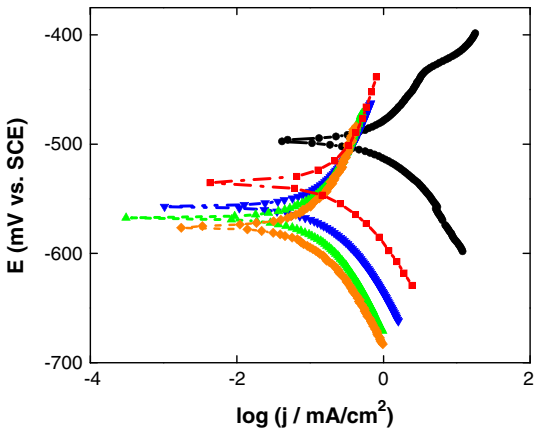

Fig. 2 Polarization curves for mild steel in 0.5 M H2SO4 without (*filled circle*) and with various concentrations of TTU [30 μM (*filled square*); 60 μM (*filled inverted triangle*); 90 μM (*filled triangle*); 120 μM (*filled diamond*)], at 30 °C

3.1.2 Potentiodynamic polarization measurements

Potentiodynamic polarization measurements were performed in the absence and presence of different concentrations of TTU in order to obtain inhibition efficiency values and to gain a deeper insight into mechanistic aspects of the inhibition process. Figure 2 shows typical potentiodynamic polarization curves measured with steel samples after 24 h immersion in 0.5 M H_2SO_4 without and with different concentrations of TTU. From Fig. 2, it can be observed that the mild steel specimen exhibits active dissolution with no distinctive transition to passivation within the studied potential range, as expected for highly acidic solutions. After inhibitor addition the following characteristic features can be clearly observed from data in Fig. 2: (i) addition of the inhibitor results in a larger slope for the anodic Tafel straight lines ba, while the cathodic Tafel slope remains invariant; (ii) the corrosion potential E_{corr} shifts towards more negative values; (iii) increasing the concentration of the inhibitor changes neither the anodic nor the cathodic Tafel slopes. These features can be

Table 2 Electrochemical parameters for the corrosion of mild steel in 0.5 M H_2SO_4 solution with and without different concentrations of inhibitors at 30 °C

TTU concentration (c) (μM)	j_{corr} (mA/cm^2)	ba (mV)	bc (mV)	Rp (Ωcm^2)	E_{corr} (mV)	$\%\eta$ [a] $_{(Rp)}$
0	1.10	78	43	11	−502	0
30	0.57	107	47	25	−525	56.0
60	0.40	102	46	34	−536	67.6
90	0.30	106	45	46	−555	76.1
120	0.27	113	51	56	−567	80.4

[a] $\%\eta_{(Rp)} = 100 \times (1- Rp°/Rp^{inh})$, where $Rp°$ and Rp^{inh} are the polarization resistances in the absence of TTU and in the presence of different concentrations of TTU, respectively

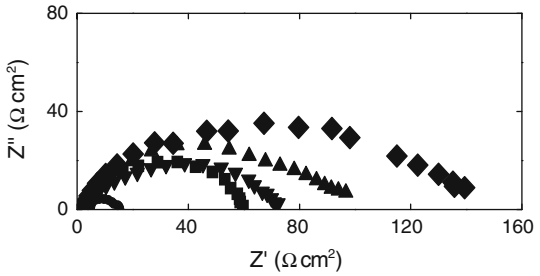

Fig. 3 Nyquist plots for mild steel in 0.5 M H2SO4 without (*filled circle*) and with different concentrations of inhibitor (30 μM (*filled square*); 60 μM (*filled inverted triangle*); 90 μM (*filled triangle*); 120 μM (*filled diamond*))

understood in terms of decreasing cathodic areas with increasing TTU concentration and a change in the oxidation reaction mechanism associated with the addition of the inhibitor. However, the anodic kinetic parameters for the metal dissolution reaction remain independent of TTU concentration. Consequently, even though TTU acts mainly as a cathodic inhibitor, when absent, the anodic mechanistic pathway is different and related to a larger value of the transfer coefficient, or put in other words, related to a less polarized electrochemical reaction.

Values for anodic and cathodic Tafel slopes, corrosion current density (j_{corr}), corrosion potential (E_{corr}), polarization resistance (Rp) and inhibition efficiency ($\%\eta$) calculated from polarization data are presented in Table 2 for test solutions without and with different concentrations of the inhibitor. j_{corr} values and Tafel slopes were determined directly from the low-overvoltage (non-Tafel) region through curve fitting [11, 12].

In agreement with weight loss measurements, there is an increase in the inhibition efficiency values as TTU concentrations increase.

3.1.3 Electrochemical impedance spectroscopy (EIS)

The corrosion behaviour of mild steel, in acidic solutions of TTU, was investigated by EIS after immersion for 24 h, at (30 ± 0.5) °C. EIS experiments were primarily performed as an independent and complementary means of determining, in a rapid and accurate way, corrosion rates for mild steel in inhibited 0.5 M H_2SO_4 solutions. The analysis was focused on how the impedance response is modified by the presence of TTU. Figure 3 shows impedance spectra represented as Nyquist plots and obtained for mild steel in the absence of TTU and in the presence of different TTU concentrations. Impedance spectra typically show a single depressed capacitive semicircle within the studied frequency range. The capacitive loop contains double layer capacitance (C_{dl}) charging effects and additionally, reflects resistive phenomena due to the charge transfer resistance R_t. In this case R_t is the single element in the Faradaic impedance of the interfacial reactions [13, 14]. Moreover, inspection of Fig. 3 reveals that addition of TTU to the corrosive medium results in a continuous increase in the size of the semicircle in the Nyquist plot for increasing concentrations of the inhibitor. This response is a clear indication of the inhibition of the corrosion process.

The system considered here is characterized by a simple corrosion process with both anodic and cathodic reactions under strict electron-transfer control and uniform corrosion on homogenous surfaces. Consequently, the impedance in this case can be described by an equivalent circuit resulting from the electrolyte resistance R_s in series connection with a parallel combination of the interfacial capacitance and the charge transfer resistance. Moreover, in studies of corroding systems, constant phase elements (CPEs) are most often used to describe the frequency dependence of nonideal capacitive behaviour. The impedance of a CPE is given by Eq. 4.

$$Z(CPE) = Y_0^{-1}(j\omega)^{-n} \tag{4}$$

with $j = \sqrt{-1}$ and $\omega = 2\ \pi\ f$, where f is the frequency of the sinusoidal perturbation signal.

Conversion of fit parameter Y_0 into C_{dl} can be performed according to the following relationship (Eq. 5) [15].

$$C_{dl} = \left(2\,\pi f_m'' R_t\right)^{-1} \tag{5}$$

where f_m'' is the frequency at which the imaginary component of the impedance is at a maximum while charge transfer resistance R_t values result from the parametric fit of the experimental spectra to the equivalent circuit equation.

The inhibition efficiency of the corrosion of steel was calculated using Eq. 6.

$$\%\eta_{EIS} = \frac{R_{t\,o}^{-1} - R_{t\,inh}^{-1}}{R_{t\,inh}^{-1}} \times 100 \quad (6)$$

where R_{to} and $R_{t\ inh}$ are the charge transfer resistance values corresponding to electrolytes without and with added inhibitor, respectively. Impedance parameters derived from this analysis are given in Table 3. Results in Table 3 show that the value of the charge transfer resistance increased in the presence of TTU when compared to the blank solution. It is also observed that R_t increases with an increase in TTU concentration which, in turn, determines an increase in $\%\eta$ values. This behaviour is the same as that observed with weight loss and polarization methods.

To show the goodness of fit of the simulation model, fitted impedance spectra are shown in Figs. 4a,b containing Nyquist and Bode plots for the sulphuric solution without added inhibitor and the sulphuric acid solution containing 30 μM TTU.

Table 3 Electrochemical impedance parameters for mild steel in 0.5 M H_2SO_4 without and with different concentration of TTU, after 24 h of immersion, at (30 ± 0.5) °C

Concentration of TTU (c) (μM)	R_t (Ohm.cm^2)	C_{dl} (μF/cm^2)	$\%\eta_{EIS}$
0	12	2,423	–
30	60	566	80
60	75	205	84
90	105	145	88
120	152	120	92

3.2 Surface morphological examination

Surface morphologies of the unexposed steel sample as well as those of samples immersed for 24 h in 0.5 M H_2SO_4 solution, in the absence and presence of 120 μM TTU at 30 °C, were examined using SEM. The results shown in Fig. 5b reveal that the mild steel specimen exhibits a very rough surface in the absence of TTU due to corrosive attack by the acid solution. In the presence of TTU (Fig. 5c) surface roughness reduces indicating the inhibiting effect of TTU. The attack was relatively uniform with slight evidence of selective corrosion (compare Fig. 5c with Fig. 5a for the unexposed mild steel).

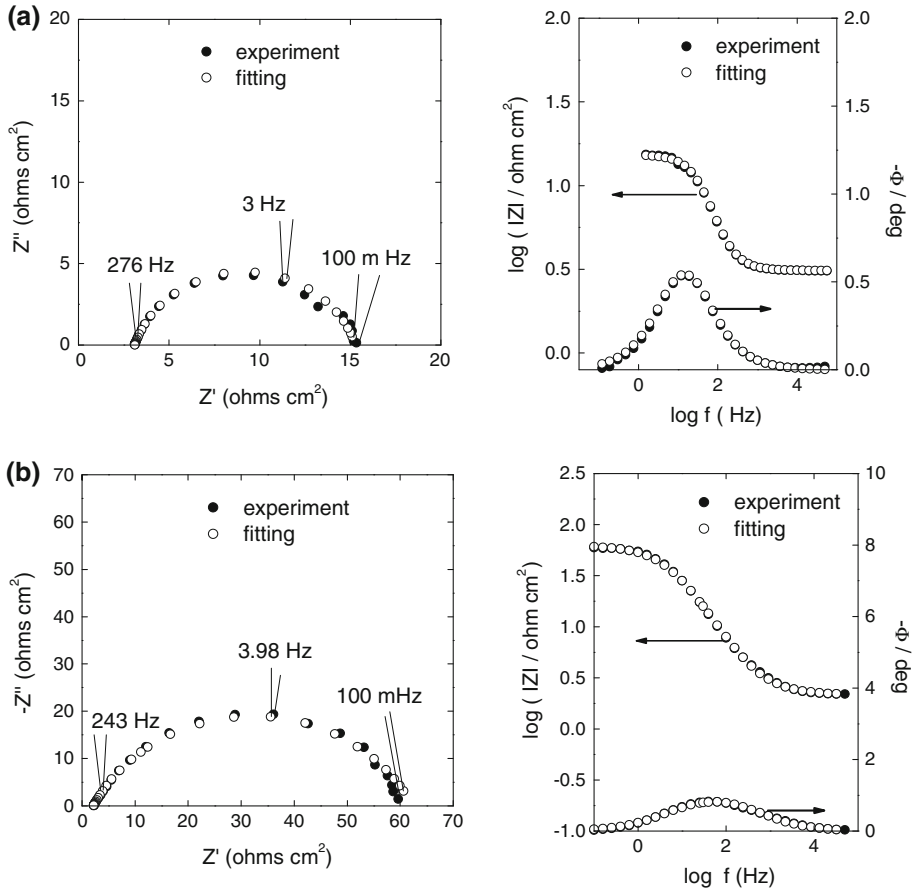

Fig. 4 Nyquist and Bode plots for mild steel in 0.5 M H2SO4 without (**a**) and with 30 μM of TTU (**b**)

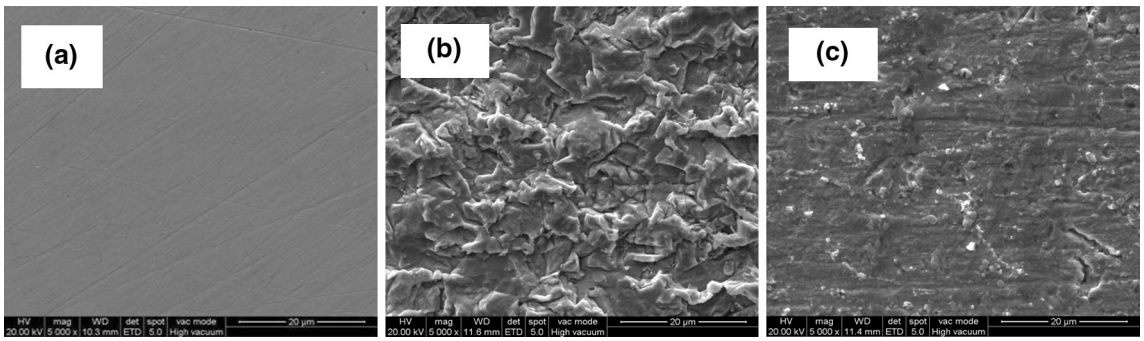

Fig. 5 SEM images (×5000) for: **a** unexposed mild steel, **b** mild steel after immersion in 0.5 M H2SO4, and **c** mild steel after immersion in 0.5 M H2SO4 containing 120 μM TTU, at 30 °C for 24 h

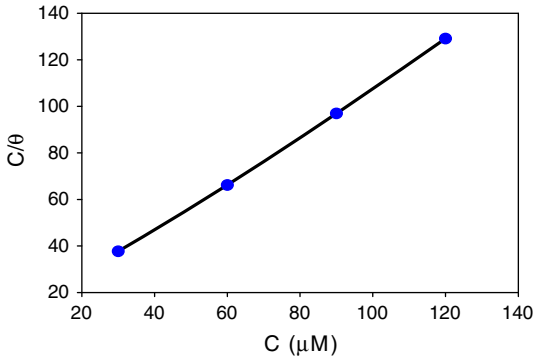

Fig. 6 Langmuir adsorption isotherm for TTU on mild steel in 0.5 M H2SO4, at 30 °C

3.3 Inhibitor adsorption

Basic information regarding the interaction between the inhibitor molecules and the mild steel surface can be provided in terms of the adsorption isotherm. Attempts were made to fit experimental data to various isotherms including Frumkin, Langmuir and Temkin models. Results were best fit to the Langmuir adsorption isotherm (Eq. 7).

$$\frac{C}{\theta} = \frac{1}{K} + C \tag{7}$$

where C is the inhibitor concentration, K is the adsorption equilibrium constant, and θ is the surface coverage (Eq. 3).

Plotting C/θ against C yields a straight line as shown in Fig. 6. Both linear correlation coefficient (r = 0.9993) and slope (1.0467) are very close to 1, indicating the adsorption of TTU on steel surface obeys the Langmuir adsorption isotherm. A large value for K (6.00×10^6 M^{-1}) was calculated. It was shown that K values larger than 100 are associated with a strong and stable adsorbed layer of inhibitor on the metal surface [16]. K is related to the standard free energy of adsorption ($\Delta G°$) according to Eq. 8.

$$K = \frac{1}{55.5}\exp\left(\frac{-\Delta G^0}{RT}\right) \tag{8}$$

where R is the gas constant (8.314 JK^{-1} mol^{-1}), T the absolute temperature (K), and the value 55.5 is the concentration of water in solution expressed in molar units.

Negative values of $\Delta G°$ are widely accepted as ensuring a spontaneous adsorption process and formation of a stable adsorbed layer on the steel surface [17–19]. In fact, ΔG rather than $\Delta G°$ has to be considered as the criterion of spontaneous change under non-standard conditions (at constant temperature and pressure) [20]. However, the easy availability of $\Delta G°$ values explains why they are usually used to get a rough idea of the direction of spontaneous change. The present study gives a value of $\Delta G° = -49.4$ $kJmol^{-1}$. Since $\Delta G°$ is not significantly negative, we can not ensure that the adsorption process will be spontaneous and virtually complete under any reasonable set of conditions.

3.4 Explanation for the inhibition process

The inhibition mechanism can be understood in terms of the adsorption of the inhibitor at the steel/solution interface. Inhibitor adsorption is related to its chemical structure, the nature and charge on the metal surface and the composition of the corrosive medium. The TTU chemical structure (Fig. 1) shows that the molecule has various possible active sites for the adsorption process. Accordingly, at least four types of adsorption involving TTU molecules on steel surface may be considered, as follows:

(i) In an acid solution a fraction of TTU molecules can be protonated. Protonation of TTU takes place at the S atom of the 1,3-imidazolidine-2-thione moiety, as indicated in Eq. (9) [21–23]. It is well known that the equilibrium position between cyclic thiamides and the tautomeric imidothiol form shifts towards the thioamide

side [24, 25].

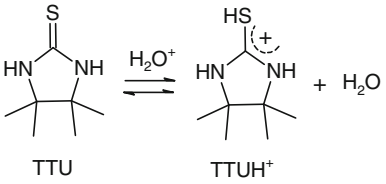

(9)

Thus in aqueous acidic solutions, protonated cations ($TTUH^+$) coexist with neutral molecules (TTU).

Considering that the potential of zero charge (E_{pzc}) for iron in 0.5 M H_2SO_4 is −550 mV vs. SCE [2, 26] and E_{corr} was measured to be −502 mV versus SCE, the steel surface is positively charged. Since SO_4^{2-} anions can adsorb specifically, they might create an excess negative charge on the metal surface and favour further adsorption of the cationic $TTUH^+$ species [27].

(ii) TTU may adsorb on the metal surface via a chemisorption mechanism that involves coordinate bonds between the lone electron pairs of the N, O and exocyclic S atoms and the vacant d-orbitals of Fe atoms. Similarly, π-electrons in the aromatic phenyls of TTU can drive adsorption through a donor–acceptor interaction.

(iii) TTU contains a thiocarbonyl group (>C=S) that represents a group of known ligands [7]. Thus, TTU may combine with freshly generated Fe^{2+} ions on the steel surface forming metal inhibitor complexes (Eqs. 10, 11). These complexes at the steel surface may form a blocking barrier to further iron dissolution.

$$Fe \rightleftarrows Fe^{+2} + 2e \tag{10}$$

$$TTU + Fe^{2+} \rightleftarrows [TTU - Fe]^{2+} \tag{11}$$

(iv) Considering the Volmer step of the well-known hydrogen evolution mechanism [28–30] protonated $TTUH^+$ may adsorb competing with hydrogen ions for the available cathodic sites and hence hinder hydrogen evolution.

4 Conclusions

(1) TTU acts as a good inhibitor for the corrosion of mild steel in 0.5 M H_2SO_4 solutions. Inhibition efficiency ($\%\eta$) increases with the inhibitor concentration, and the maximum $\%\eta$ value is 93.4 % for 120 μM TTU.

(2) In sulfuric acid media, the adsorption of TTU obeys the Langmuir adsorption isotherm. The standard free energy ($\Delta G°$) is not large enough to consider that the adsorption of TTU will be spontaneous and complete under every reasonable composition of the system.

(3) TTU acts as a cathodic-type inhibitor in 0.5 M H_2SO_4, since it primarily retards the cathodic reaction.

(4) Different mechanisms for the adsorption of TTU must be considered since the following alternatives are possible: electrostatic attraction between anions (SO_4^{2-}) and protonated inhibitor molecules, sharing of electrons between the N, S and O atoms and Fe, donor–acceptor interactions between π-electrons of aromatic rings and vacant d-orbitals of Fe and adsorption of complexes of the type $[TTU\text{-}Fe]^{2+}$.

Acknowledgments C.A. Gervasi gratefully acknowledges the Comisión de Investigaciones Científicas y Técnicas Buenos Aires (CICBA) for his position as a member of the Carrera del Investigador Científico. This work was partially financed with a grant from Agencia Nacional de Promoción Científica y Tecnológica (PICT N° 2008-1902), and M.V. Mirífico gratefully acknowledges to the Consejo Nacional de Investigaciones Científicas y Técnicas (CONICET) (PIP 0847), Universidad Nacional de La Plata (UNLP), and Facultad de Ingeniería UNLP, Área Departamental de Ingeniería Química (11-I162).

References

1. ASM Metal Handbook (1994) In: Reidenbach F (ed) Surface Engineering, vol 4, 10th edn. ASM International, Metals Park
2. Li X, Deng S, Fu H (2011) Triazolyl blue tetrazolium bromide as a novel corrosion inhibitor for steel in HCl and H_2SO_4 solutions. Corros Sci 53:302–309
3. Bentiss F, Lagrenee M, Traisnelb M, Hornez JC (1999) The corrosion inhibition of mild steel in acidic media by a new triazole derivative. Corros Sci 41:789–803
4. Granese SL, Rosales BM, Oviedo C, Zerbino JO (1992) The inhibition action of heterocyclic nitrogen organic compounds on Fe and steel in HCl media. Corros Sci 33:1439–1453
5. Mirífico MV, Caram JA, Vasini EJ, Piro OE, Castellano EE (2009) Reactions of 1,2,5-thiadiazole 1,1-dioxide derivatives with nitrogen nucleophiles. Part IV. Addition of α-diamines. J Phys Org Chem 22(2):163–169
6. Kazak C, Yılmaz VT, Servi S, Koca M, Heinemann FW (2005) 1,3-Dibenzoylimidazolidine-2-thione and 1,3- dibenzoyl-3,4,5,6-tetrahydropyrimidine-2(1H)-thione. Acta Crystallogr C 61(6):348–350
7. Raper ES (1985) Complexes of heterocyclic thione donors. Coord Chem Rev 61:115–184
8. Hussain MS, Al–Arfaj AR, Hossoin ML (1990) Mixed-ligand complexes of copper(I) with heterocyclic thiones. Transit Met Chem 15:264–269
9. Bincy J, Sam J, Abraham J, Narayana B (2010) Imidazolidine-2-thione as corrosion inhibitor for mild steel in hydrochloric acid. Indian J Chem Technol 17:366–374
10. Umoren SA (2011) Synergistic inhibition effect of polyethylene glycol—polyvinyl pyrrolidone blends for mild steel corrosion in sulphuric acid medium. J Appl Polym Sci 119: 2072–2084
11. Jones DA (1992) In: Johnstone D (ed) Principles and prevention of corrosion. Macmillan Publishing Company, New York
12. Mansfeld F (1973) Tafel slopes and corrosion rates from polarization resistance measurements. Corrosion 29:397–402
13. Abd El Rehim SS, Hassan HH, Amin MA (2001) Corrosion inhibition of aluminum by 1,1(lauryl amido)propyl ammonium chloride in HCl solution. Mater Chem Phys 70:64–72
14. Khaled KF, Al-Qahtani MM (2009) The inhibitive effect of some tetrazole derivatives towards Al corrosion in acid solution: chemical, electrochemical and theoretical studies. Mater Chem Phys 113:150–158

15. Hsu CH, Mansfeld F (2001) Concerning the conversion of the constant phase element parameter Y_0 into a capacitance. Corrosion 57:747–748
16. Lagrenée M, Mernari B, Bouanis M, Traisnel M, Bentiss F (2002) Study of the mechanism and inhibiting efficiency of 3,5-bis(4-methylthiophenyl)-4H-1,2,4-triazole on mild steel corrosion in acidic media. Corros Sci 44:573–588
17. Yurt A, Bereket G, Kivrak A, Balaban A, Erk B (2005) Effect of schiff bases containing pyridyl group as corrosion inhibitors for low carbon steel in 0.1 M HCl. J Appl Electrochem 35:1025–1032
18. Khamis E, Bellucci F, Latanision RM, El-Ashry ESH (1991) Acid corrosion inhibition of nickel by 2-(triphenosphoranylidene) succinic anhydride. Corrosion 47:677–686
19. Donahue FM, Nobe K (1965) Theory of organic corrosion inhibitors: adsorption and linear free energy relationships. J Electrochem Soc 112:886–891
20. Umoren SA, Banera MJ, Alonso-Garcia T, Gervasi CA, Mirífico MV (2013) Inhibition of mild steel corrosion in HCl solution using chitosan. Cellulose 20:2529–2545
21. Streitweiser A Jr (1961) Molecular orbital theory for organic chemistry. Wiley, New York
22. Walter W, Voss J (1970) In: Zabick J (ed) In the chemistry of amides. Interscience, New York, p 187
23. Pillai KC, Narayan R (1978) Inhibition of corrosion of iron in acids by thiourea and derivatives. J Electrochem Soc 125(9):1393–1397
24. Sandström J, Wennerbeck I (1966) Tautomeric cyclic thiones, Part II. Acta chem Scand 20:57–61
25. Caram JA, Mirífico MV, Aimone SL, Piro OE, Castellano EE, Vasini EJ (2004) The addition reaction of diamides to 1,2,5-thiadiazole 1,1-dioxide derivatives. J Phys Org Chem 17(12):1091–1098
26. Roy SC, Roy SK, Sircar SC (1988) Critique of inhibitor evaluation by polarization measurement. Br Corros J 32:102–104
27. Bentiss F, Traisnel M, Lagrenée M (2000) The substituted 1,3,4-oxadiazoles: a new class of corrosion inhibitors of mild steel in acidic media. Corros Sci 42:127–146
28. Subramanyan PK (1981) In: Bockris JO'M, Conway BE, Yeager E, White RE (eds) Comprehensive treatise of electrochemistry, vol 4. Plenum Press, New York, pp 411–459
29. Tilak BV, Chen CP, Rangarajan SK (1992) A model to characterize the impedance of electrochemical capacitors arising from reactions of the type $O_{ad} + ne^- \leftrightarrow R_{ad}$. J Electroanal Chem 324:405–414
30. Bockris JO'M, Khan SUM (1993) Surface electrochemistry, a molecular level approach. Plenum Press, New York, pp 211–394